



Influence of substrate on molecular order for self-assembled adlayers of CoPc and FePc

Abhishek Kumar^{1,2}  | Denys Naumenko³ | Luca Cozzarini¹ | Luisa Barba⁴ | Alberto Cassetta⁴ | Maddalena Pedio¹ 

¹Istituto Officina dei Materiali, Consiglio Nazionale delle Ricerche, TASC Laboratory, Trieste, Italy

²Dipartimento di Fisica, Università di Trieste, Trieste I-34127, Italy

³Elettra Sincrotrone Trieste, Area Science Park Basovizza, Trieste 34149, Italy

⁴Istituto di Cristallografia, Consiglio Nazionale delle Ricerche, S.S. 14, Km 163, 5 Basovizza, Trieste 34149, Italy

Correspondence

Abhishek Kumar, Istituto Officina dei Materiali, Consiglio Nazionale delle Ricerche, TASC Laboratory, Trieste, Italy. Email: abhishek.puchd@gmail.com

Funding information

NFFA European Union's Horizon 2020 research and innovation programme, Grant/Award Number: 654360; EUROFEL MIUR Progetti Internazionali

Abstract

Self-assembled metal phthalocyanine thin films are receiving considerable interest due to their potential technological applications. In this study, we present a comprehensive study of CoPc and FePc thin films of about 50 nm thickness on technologically relevant substrates such as SiO_x/Si, indium tin oxide (ITO) and polycrystalline gold in order to investigate the substrate induced effects on molecular stacking and crystal structure. Raman spectroscopic analysis reveals lower intensity for the vibrational bands corresponding to phthalocyanine macrocycle for the CoPc and FePc thin films grown on ITO as compared to SiO_x/Si due to the higher order of phthalocyanine molecules on SiO_x/Si. Atomic force microscopy analysis displays higher grain size for FePc and CoPc thin films on ITO as compared to SiO_x/Si and polycrystalline gold indicating towards the influence of molecule–substrate interactions on the molecular stacking. Grazing incidence X-ray diffraction reciprocal space maps reveal that FePc and CoPc molecules adopt a combination of herringbone and brickstone arrangement on SiO_x/Si and polycrystalline gold substrate, which can have significant implications on the optoelectronic properties of the films due to unique molecular stacking.

KEYWORDS

metal phthalocyanine thin films, molecular stacking, molecule–substrate interactions, Raman spectroscopic analysis

1 | INTRODUCTION

Transition metal phthalocyanines (MPc) are the peculiar class of organic molecules, which due to their unique electrical and magnetic properties have the potential for optoelectronic and spintronic applications.^[1] The properties of MPc are strongly influenced by polymorphism, crystal structure, and central metal atom.^[1,2] In recent years, considerable progress has been made in understanding the self-assembly of these molecules on metallic substrates with the aim to demonstrate interfacial electronic

properties. Moreover, due to their thermal stability at elevated temperatures, these molecules have been explored for their application in organic field-effect transistors and solar cells.^[3,4] In view of impactful applications, it is crucial to obtain detailed information about the surface topography and preferred orientation of the crystallites. In addition, nature of substrate significantly influences the properties of the MPc thin films by controlling the molecular orientation during growth.^[5]

The relative orientation of the molecules is driven by the fine interplay between molecule–substrate interactions

and intermolecular forces and thus controls the molecular and optoelectronic properties of the system.^[5]

MPC thin films show different polymorphism depending on growth conditions and nature of substrate exhibiting triclinic or monoclinic symmetries.^[6] Surface properties of the substrate can significantly influence the growth mechanism and effectively control the crystal phase and film structure.^[7] The molecular arrangements of polymorphs influence the optical and transport properties of thin films significantly. It has been demonstrated that the absorption spectrum of MPC is red shifted in the triclinic structure due to increased intermolecular interactions in this phase.^[8] In order to gain control over the organic thin films phase and morphology, organic molecular beam deposition has been effectively utilized to get good reproducibility. In addition, the interaction of the central metal atom with substrate effectively controls the organic thin films properties as the hybridization of metal 3d and macrocycle orbitals determine the energy separation between highest occupied molecular orbital and lowest unoccupied molecular orbital, which is a crucial parameter for optoelectronic devices.^[8]

Micro Raman scattering spectroscopy has been utilized to study the polymorphism of CoPc and FePc on silicon at different growth temperatures.^[9] CoPc and FePc thin films show phase transition from α polymorph to β polymorph above 200 °C, and polarized Raman spectroscopy efficiently distinguishes the two phases. However, a comprehensive study for the room temperature deposition of FePc and CoPc on technologically relevant substrates is lacking. X-ray absorption spectroscopy-based study for the adsorption of CuPc on polycrystalline gold and indium tin oxide (ITO) shows that molecules adopt standing configuration on the substrates.^[10] However, detailed molecular arrangements have not been thoroughly understood. A multitechnique characterization approach is needed to gain the detailed information about the molecular phases. We have adopted grazing incidence X-ray diffraction (GIXRD), atomic force microscopy (AFM), and Raman spectroscopy to study the solid state packing of MPC on three technologically significant substrates.

2 | EXPERIMENTAL SECTION

Thin films of CoPc and FePc of about 50 nm thickness were deposited on ITO (1.7 nm roughness), polycrystalline gold (Au, 0.3 nm roughness), and native oxide SiO_x on Si(100) (SiO_x roughness is 0.2 nm). The FePc and CoPc high purity polycrystalline powders (Sigma Aldrich) were evaporated from resistively heated quartz

crucibles in UHV at the base pressure of 2×10^{-10} mbar and low deposition rate of 2 Å/min. All the depositions were performed at room temperature. The three substrates were rinsed in acetone before introducing them into the UHV chamber.

GIXRD measurements were performed at the X-ray Diffraction beamline 5.2 at the Synchrotron Radiation Facility Elettra in Trieste, Italy. The beam was monochromatized at 1.4 Å. The samples were oriented by means of a four-circle diffractometer following the standard procedures.^[11] Bidimensional diffraction patterns were recorded with a 2M Pilatus silicon pixel X-ray detector (DECTRIS Ltd.) positioned perpendicular to the incident beam, at a distance of 130 mm from the sample. The sample inclination to the beam was about 1°, well over the critical angle for total external reflection of the substrate. Patterns were calibrated by means of a LaB₆ standard and integrated using the software Fit2D,^[12] obtaining several series of powder like patterns, corrected for geometry, Lorentz and beam polarization effects. The 2theta range was spanned from 0.1° to 44.2° with resolution of 1.85 Å. Peaks positions were extracted by means of Fit2D in association with WinPLOT.^[13]

The Raman measurements were performed in the reflection geometry. Continuous wave laser with a wavelength of 532 nm (Cobolt Samba, 50 mW, bandwidth 1 MHz) was used as excitation source. The 532 nm RazorEdge Dichroic™ laser-flat beam splitter and 532 nm RazorEdge® ultrasteep long-pass edge filter were used to direct the light into the microscope (Axiovert 200, Zeiss) and cut Rayleigh scattered light before the spectrometer (Shamrock SR-750, Andor Technology plc.) respectively. The laser power on the sample was controlled by the neutral density filter (Thorlabs) and kept at 100 μW. The acquisition time in all experiments was 600 s.

AFM measurements were performed in contact mode using Nanowizard II AFM (JPK), which allows scanning the sample in the range of 100 × 100 × 15 μm. CSG 01 Silicon probes (NT-MDT) with a force constant of 0.05 N/m and 10 nm tip curvature were used.

3 | RESULTS

Figure 1 shows the 2D GIXRD reciprocal space maps for the deposition of the 50-nm-thick CoPc and FePc films on polycrystalline gold, SiO_x/Si, and ITO substrates. Reciprocal space maps show significant structural differences between depositions for the same molecule on three substrates. As shown in Figure 1a,d, the reciprocal space maps for the deposition of CoPc and FePc on

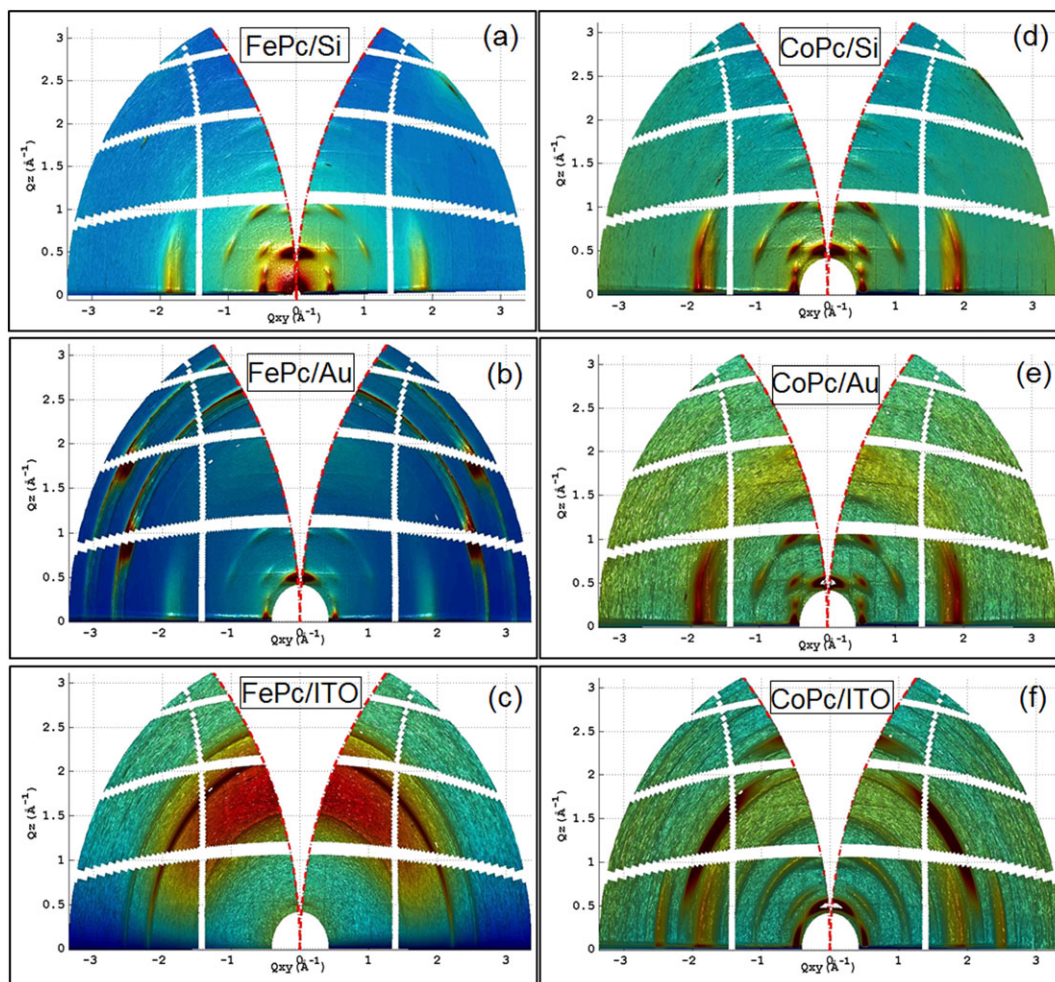


FIGURE 1 Grazing incidence X-ray diffraction (GIXRD) reciprocal space maps for the deposition of ((a)–(c)) FePc and ((d)–(f)) CoPc on SiO_x/Si, Au, and ITO at room temperature. ITO = indium tin oxide [Colour figure can be viewed at wileyonlinelibrary.com]

SiO_x/Si exhibit multiple diffraction spots depicting highly crystalline and ordered structure. However, in case of polycrystalline Au, the diffraction spots are comparatively spread demonstrating that crystalline order is less pronounced on Au as compared to SiO_x/Si. It suggests that the FePc and CoPc crystallites disperse over a range of orientations and single stacking is not present. The comparison of reciprocal space maps for the CoPc and FePc deposition on SiO_x/Si and ITO unambiguously shows almost no detectable diffraction spots on ITO. This confirms that crystalline order is poor and MPC molecules are randomly oriented on ITO. The reciprocal space maps for the deposition of FePc and CoPc on SiO_x/Si show good resemblance with the reciprocal space maps for CuPc adsorbed on ZnO(1 $\bar{1}$ 00).^[14] The peaks observed around $Q_{xy} = 1.7, 1.9 \text{ \AA}^{-1}$ and $Q_{xy} = 0.5, 1.04 \text{ \AA}^{-1}$ are assigned to brickstone (100) oriented phase and herringbone (200) oriented phase, respectively.^[14] The observation of diffraction spots at similar values of Q_{xy} suggests that for 50-nm-thick CoPc and FePc films, the molecules are arranged in a mixed

phase. Although peaks are observed around $Q_{xy} = 1.7, 1.9 \text{ \AA}^{-1}$ and $Q_{xy} = 0.5, 1.04 \text{ \AA}^{-1}$ for the deposition of CoPc and FePc on Au substrate, diffraction spots appear less intense and tend to disperse as compared to SiO_x/Si due to reduced molecular order on polycrystalline Au.

Peak profile analysis has been performed after indexing the patterns, by the Hosemann model.^[15] The paracrystallinity analysis in Table S1 has been performed for the out of plane (OOP) direction assign similar paracrystallinity parameters for FePc thin films deposited on SiO_x/Si, Au, and ITO. This suggests that the molecular order does not differ significantly within domains, even though overall crystalline order is poor for deposition on ITO as compared to SiO_x/Si and Au. The paracrystallinity analysis has been performed for herringbone and brickstone phases, identified on diffraction patterns of CuPc deposition on ZnO(1 $\bar{1}$ 00) by means of the SimDiffraction simulation software.^[16] Importantly, the analysis assigns nearly the same values for the two phases suggesting that herringbone and brickstone phases exhibit almost similar molecular order

within domains. Paracrystallinity analysis performed for the in-plane (IP) direction reported in Table S1 assigns lower paracrystallinity parameters as compared to OOP direction for FePc and CoPc deposition on Au and SiO_x/Si indicating higher crystalline order within domains along the IP direction. Peak profile analysis shows that crystallites along OOP (i.e., in the h00) direction have larger dimensions but lower crystallinity than those in the IP direction. In the first case, arrangements of the molecules organized in not too rigidly bound columnar structures are the probable causes of the high value of the paracrystallinity parameter. However, in the second case, molecules arrange edge-on with respect to the substrate and display better molecular order with a much lower paracrystallinity value. However, such arrangements of the molecules are more difficult to maintain in the long range, which results in smaller dimensions of the crystallites. Crystallite sizes reported in Table S1 are related to the coherence length in the specified crystallographic direction.

We have analyzed the topography of CoPc and FePc thin films using AFM as shown in Figure 2. FePc films on Au consist of densely packed, small elongated grains, which are randomly distributed. Notably, the grain density for the FePc thin film on Au is higher as compared to that of CoPc thin film on Au. These grains have good resemblance with CuPc thin films grains deposited on the glass which adopts α -phase for room temperature deposition.^[17] The shape of grains is characteristic of α -phase as β -phase exhibits much longer grain size obtained for the deposition above 200 °C temperature.^[15] AFM images were analyzed using average crystallite size and root mean square (RMS) parameters as listed in Table 1. The average crystallite size and RMS values are highest for ITO as compared to Au and SiO_x/Si. Lower RMS

values for the deposition of FePc and CoPc on Au and SiO_x/Si indicate that molecules are uniformly distributed as compared to ITO. Due to weaker interactions of FePc and CoPc with ITO, the molecules tend to aggregate under the influence of intermolecular interactions, which results in higher surface roughness and average crystallite size. Scanning tunneling microscopy (STM) study for the room temperature deposition of FePc on Au(111) shows that molecules adopt columnar stacking structure on Au(111). The molecules lie on the substrate with small tilt angle at low film thickness due to higher molecule–substrate interactions.^[18] It is the strength of molecule–substrate and molecule–molecule interactions that generally control the self-assembly of the molecules and first layer may direct the orientation of further layers. Comparatively lower crystallite size and RMS values for deposition of FePc and CoPc on Au and SiO_x/Si indicate that the influence of molecule–substrate interactions appear to be more pronounced for Au and SiO_x/Si as compared to ITO and significantly influence the film growth. Average crystallite size (surface and volume weighted) obtained by the GIXRD peak profile analysis agrees reasonably with the values obtained from AFM image analysis (Table 1) and follows a similar trend. Due to the poor crystalline order for the deposition of CoPc on ITO, the peak profile analysis could not be performed that is displayed in Table 1.

The Raman spectra of CoPc and FePc thin films of about 50 nm thickness deposited on Au, SiO_x/Si, and ITO are shown in Figures 3 and 4. All spectra are normalized to the intensity of vibrational mode at 1,532 cm⁻¹ and shifted vertically for clarity. No background subtraction was performed. The assignments of the peaks related to various vibrational modes are shown in Figures 3 and 4.^[19–21] No significant

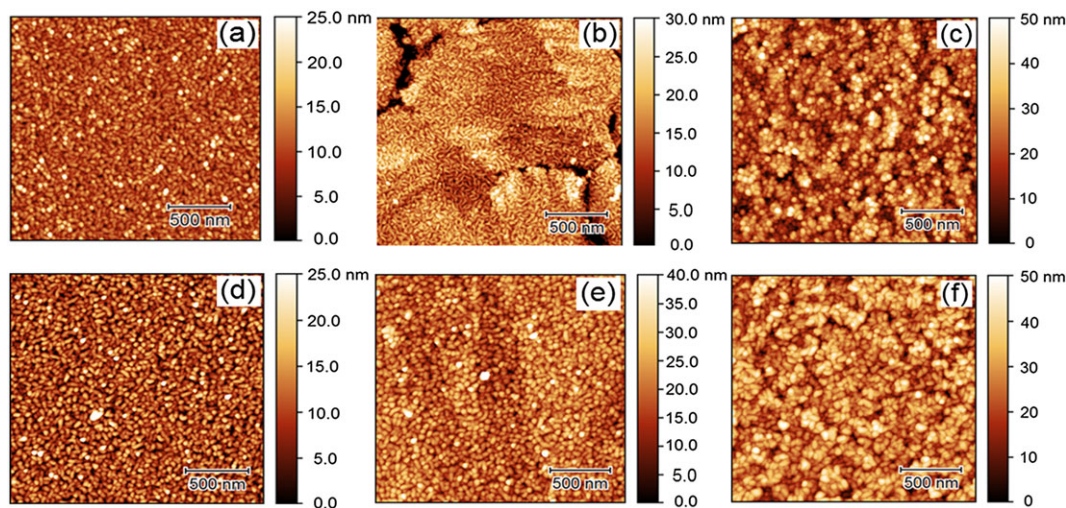
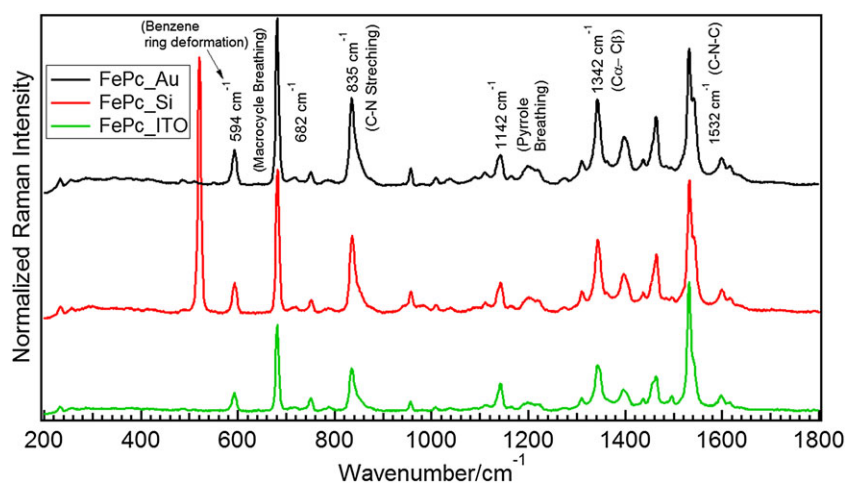
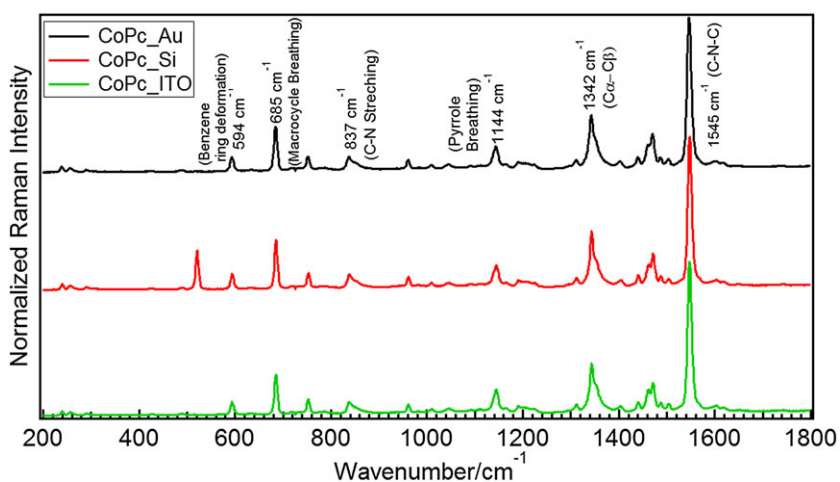


FIGURE 2 Atomic force microscopy images for the deposition of ((a)–(c)) FePc and ((d)–(f)) CoPc on SiO_x/Si, Au, and ITO at room temperature. ITO = indium tin oxide [Colour figure can be viewed at wileyonlinelibrary.com]

TABLE 1 Average grain size as obtained from atomic force microscopy (AFM) analysis compared with the crystallite size as obtained from grazing incidence X-ray diffraction (GIXRD) peak profile analysis

System	Average grain size (AFM analysis; nm)	RMS (roughness; nm)	Average crystallite surface weighted size (GIXRD; nm)	Average crystallite volume weighted size (GIXRD; nm)
FePc_SiO _x /Si	10.5	3.2	12.0	11.8
FePc_Au	17.8	3.4	16.9	14.0
FePc_ITO	20.8	8.8	18.0	17.3
CoPc_SiO _x /Si	10.7	4.5	12.4	12.0
CoPc_Au	18.5	5.1	14.0	13.1
CoPc_ITO	23.9	7.5	No data	No data

FIGURE 3 Raman spectrum of FePc films on polycrystalline Au, SiO_x/Si, and ITO. ITO = indium tin oxide substrates [Colour figure can be viewed at wileyonlinelibrary.com]**FIGURE 4** Raman spectrum of CoPc films on polycrystalline Au, SiO_x/Si, and ITO substrates. ITO = indium tin oxide [Colour figure can be viewed at wileyonlinelibrary.com]

wavenumber shifts are observed for the Raman vibrational bands of CoPc and FePc deposited on these substrates. In general, the Raman spectrum of MPc is dominated by A_{1g} , B_{1g} , B_{2g} , and E_g modes corresponding to vibrations of the macrocycle, isoindole moieties, and metal–nitrogen bands.^[21] The Raman bands in the 600 to 800 cm^{-1} range for both FePc and CoPc films are associated with phthalocyanine macrocycle vibrational modes, and their relative

intensities can be used to distinguish between polymorphic phases.^[22] We measured the Raman spectra of FePc α and β powders and compared them with the spectrum of FePc thin film on Au as shown in Figure 5, in order to demonstrate the type of phase adopted by FePc thin films. The spectra are normalized and shifted vertically in order to demonstrate the variation in the relative intensities of vibrational modes at 684 and 750 cm^{-1} . The α -phase

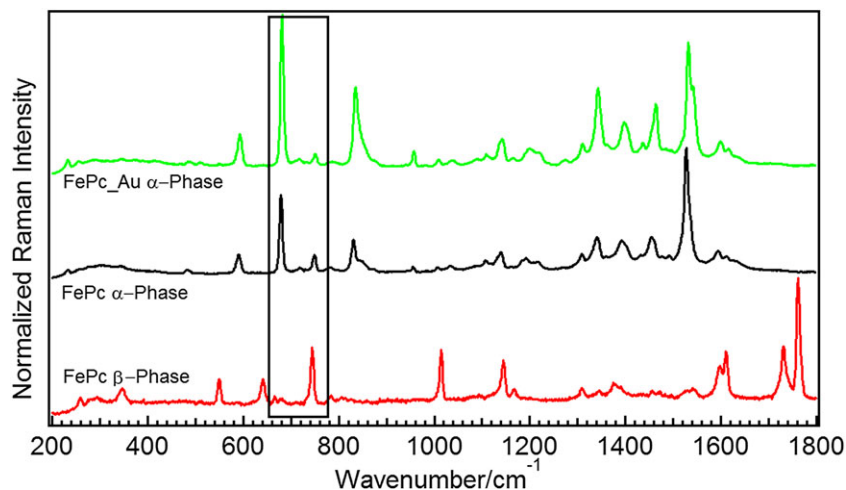


FIGURE 5 Raman spectrum of the FePc α and β crystalline powders along with α -phase FePc thin film on Au [Colour figure can be viewed at wileyonlinelibrary.com]

spectra are normalized to the intensity of vibrational mode at about $1,532\text{ cm}^{-1}$, while β -phase spectrum is normalized to vibrational mode at about $1,761\text{ cm}^{-1}$. The relative intensity of the peak at about 750 cm^{-1} for FePc α -powder is lower than the peak at about 684 cm^{-1} while the intensity ratio is reversed for β -phase.^[22] In case of FePc thin film deposited on Au, the intensity of the peak at about 750 cm^{-1} is significantly larger than at about 684 cm^{-1} testifying that thin film adopts α -phase. In addition, considerable modifications for the vibrational Raman bands are observed for the bulk powders α and β -phase as compared to thin films α -phase showing the influence of unique molecular stacking.

In order to investigate the molecular stacking of self-assembled thin films of CoPc and FePc, we have monitored the intensity of mode corresponding to macrocycle breathing vibration at 685 cm^{-1} as this mode most probably is influenced by intermolecular interactions. Figure 6 shows the variation of this mode with respect to film roughness as obtained from AFM analysis (Table 1). In order to study intensity variation, the values of the macrocycle breathing mode intensities for the deposition of CoPc and FePc on SiOx/Si, Au, and ITO are extracted from normalized spectra shown in Figures 3 and 4. The intensity of the macrocycle breathing mode is minimum for the deposition of FePc and CoPc on ITO. The intensity variation follows the trend of surface roughness in case of CoPc deposition while for the FePc deposition on Au it shows maximum value. Surface roughness, lattice structure, and chemical interaction between adsorbed molecules and substrate are the factors influencing molecular orientation and films growth.^[23] X-ray absorption studies showed that MPc molecules tend to adopt a standing configuration with increasing substrate roughness.^[23] As the intensity of Raman bands depends on crystal orientation and polarization geometry,^[24] we can associate the intensity variation of the macrocycle

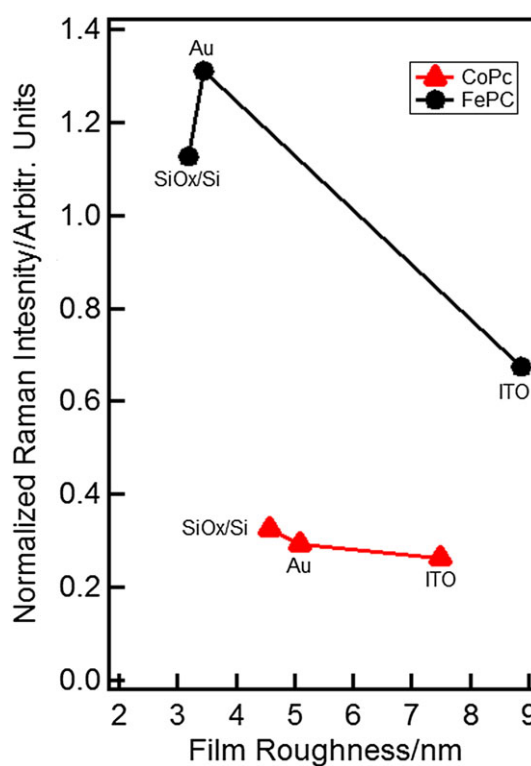


FIGURE 6 Variation of macrocycle breathing mode normalized intensity with film roughness [Colour figure can be viewed at wileyonlinelibrary.com]

breathing mode to the average molecular orientation. Due to the higher surface roughness of ITO and weaker chemical interaction as compared to SiO_x/Si and Au, disordered, standing configuration of molecules can be expected. Moreover, in the absence of stronger molecule-substrate interactions, weaker intermolecular interactions dominate and molecules adopt standing configuration.^[25] Comparatively higher Raman intensity for the deposition of FePc on Au as compared to CoPc in

Figure 6 can be associated with the different interaction with the substrate and growth mechanism induced by the different central metal atom. Importantly, dissimilarity in the FePc and CoPc growth mechanism on Au is evident from AFM analysis (Figure 2); FePc grains are elongated and dense as compared to spherical CoPc grains. In the case of the deposition of CuPc on Au, it has been observed that molecules adopt lying configuration with respect to the substrate during initial growth of the first few layers due to the higher interaction of π electron cloud with the metallic substrate.^[26] However, for the deposition on ITO, it is not expected that CoPc molecules adopt lying configuration in the absence of stronger molecule–substrate interactions. In addition, AFM analysis shows that grain size and surface roughness are relatively higher for ITO as compared to Au and SiO_x/Si. Thus, we can associate the observed variation in the macrocycle breathing mode intensity to the unique molecular orientation adopted by CoPc and FePc molecules under the influence of molecule–substrate interactions, substrate roughness, and lattice structure.

4 | CONCLUSIONS

In summary, the structural properties of FePc and CoPc film of 50 nm thickness deposited on Au, SiO_x/Si, and ITO substrates have been studied by GIXRD, revealing the coexistence of herringbone and brickstone arrangements in ordered crystallites, whose dimensions and morphologies depend on the substrate and central atom. Moreover, GIXRD analyses reveal that CoPc and FePc thin films deposited on ITO are the least ordered. Raman spectroscopic analysis shows that the macrocycle breathing mode of FePc and CoPc is sensitive to the molecular stacking in the films that is influenced by an interaction of the central metal atom with the substrate and substrate roughness. Our achievements can help a better understanding of the topography and structure of MPc films, which have significant implications for their magnetic and optoelectronic properties.

ACKNOWLEDGEMENTS

This work has been partly performed in the framework of the EUROFEL project within the Porgetti Internazionali funded by the Ministero Italiano Università e Ricerca (MIUR). L. C. acknowledges the EU-H2020 research and innovation programme under grant agreement 654360 NFFA-Europe. The technical staff of CNR-IOM Federico Salvador, Paolo Bertoch, Andrea Martin, Alexander De Luisa, and Davide Benedetti is kindly acknowledged.

ORCID

Abhishek Kumar  <http://orcid.org/0000-0002-9452-7051>

Maddalena Pedio  <http://orcid.org/0000-0002-3305-4318>

REFERENCES

- [1] J. Bartolomé, C. Monton, I. K. Schuller, *Molecular magnets physics and applications*, Springer, Berlin **2014**.
- [2] C. Defeyt, P. Vandenabeele, B. Gilbert, J. Van Pevenage, R. Cloots, D. Strivay, *J. Raman Spectrosc.* **2012**, *43*, 1772.
- [3] C. W. Tang, S. A. Vanslyke, *Appl. Phys. Lett.* **1987**, *51*, 913.
- [4] F. Carpi, D. De Rossi, *Opt. Laser Technol.* **2006**, *38*, 292.
- [5] A. O. F. Jones, B. Chattopadhyay, Y. H. Geerts, R. Resel, *Adv. Funct. Mater.* **2016**, *26*, 2233.
- [6] M. Ashida, N. Uyeda, E. Suito, *Bull. Chem. Soc. Jpn.* **1966**, *39*, 2616.
- [7] H. Peisert, X. Liu, D. Olligs, A. Petr, L. Dunsch, T. Schmidt, T. Chassé, M. Knupfer, *J. Appl. Phys.* **2004**, *96*, 4009.
- [8] K. Vasseur, K. Broch, D. Cheyns, *ACS Appl. Mater. Interfaces* **2013**, *5*, 8505.
- [9] M. Szybowski, W. Bała, S. Dümecke, K. Fabisiak, K. Paprocki, M. Drozdowski, *Thin Solid Films* **2011**, *520*, 623.
- [10] H. Peisert, T. Schwieger, J. M. Auerhammer, M. Knupfer, M. S. Golden, J. Fink, P. R. Bressler, M. Mast, *J. Appl. Phys.* **2001**, *90*, 466.
- [11] A. Lausi, M. Polentarutti, S. Onesti, J. R. Plaisier, E. Busetto, G. Bais, L. Barba, A. Cassetta, G. Campi, D. Lamba, *Eur. Phys. J. Plus.* **2015**, *130*, 1.
- [12] A. P. Hammersley, S. O. Svensson, A. Hanfland, A. N. Fitch, D. Hausermann, *High Pressure Res.* **1996**, *14*, 235.
- [13] T. Roisnel, J. R. Carvajal, *Mater. Sci. Forum* **2001**, *378*, 118.
- [14] A. C. Cruickshank, C. J. Dotzler, S. Din, S. Heutz, M. F. Toney, M. P. Ryan, *J. Am. Chem. Soc.* **2012**, *134*, 14302.
- [15] G. Scavia, L. Barba, G. Arrighetti, S. Milita, W. Porzio, *Eur. Polym. J.* **2012**, *48*, 1050.
- [16] D. Breiby, W. Bunk, H. T. Lemke, *J. Appl. Crystallogr.* **2008**, *41*, 262.
- [17] M. Krzywiecki, L. Grzadziel, *J. Phys. D: Appl. Phys.* **2014**, *47*, 335304.
- [18] F. Bartolomé, O. Bunău, L. M. García, C. R. Natoli, M. Piantek, J. I. Pascual, I. K. Schuller, T. Gredig, F. Wilhelm, A. Rogalev, J. Bartolomé, *J. Appl. Phys.* **2015**, *117*, 735.
- [19] C. Jennings, R. Aroca, A. -M. Hor, R. O. Loutfy, *J. Raman Spectrosc.* **1984**, *15*, 34.
- [20] D. R. Tackley, G. Dent, W. E. Smith, *Phys. Chem. Chem. Phys.* **2001**, *3*, 1419.
- [21] R. Prabakaran, R. Kesavamoorthy, G. L. N. Reddy, F. P. Xavier, *Phys. Stat. Sol.* **2002**, *229*, 1175.
- [22] S. Heutz, S. M. Bayliss, R. L. Middleton, G. Rumbles, T. S. Jones, *J. Phys. Chem. B* **2000**, *104*, 7124.
- [23] H. Peisert, I. Biswas, M. Knupfer, T. Chassé, *Phys. Status Solidi Basic Res.* **2009**, *246*, 1529.

- [24] M. Szybowicz, J. Makowiecki, *J. Mater. Sci.* **2012**, *47*, 1522.
- [25] H. Peisert, I. Biswas, L. Zhang, M. Knupfer, M. Hanack, D. Dini, D. Batchelor, T. Chasse, *Surf. Sci.* **2006**, *600*, 4024.
- [26] I. Biswas, H. Peisert, M. Nagel, M. B. Casu, S. Schuppler, P. Nagel, E. Pellegrin, T. Chassé, *J. Chem. Phys.* **2007**, *126*, 174704.

SUPPORTING INFORMATION

Additional Supporting Information may be found online in the supporting information tab for this article.